Proceeding Paper

Fiber Laser Cutting of AISI 431 Martensitic Stainless Steel: An Experimental Investigation †

Balasubramaniyan Chandrasekaran [1,*], Rajkumar Kaliyamoorthy [2], Anandasimhan Murugavel [1], Gokul Vinayagam [1], Ehasanulla NoorMohammed [1] and Syed Hidayathullah Karimullah [1]

1 Department of Mechanical Engineering, Sri Venkateswaraa College of Technology, Chennai 602105, India; anandasimhan@gmail.com (A.M.); tjgokul78@gmail.com (G.V.); ehasanulla2468@gmail.com (E.N.); syedhidayathullah55059@gmail.com (S.H.K.)

2 Department of Manufacturing Engineering, College of Engineering-Guindy, Anna University, Chennai 600025, India; rajkumark@annauniv.edu

* Correspondence: pvrbala@gmail.com; Tel.: +91-9865377205

† Presented at the International Conference on Processing and Performance of Materials, Chennai, India, 2–3 March 2023.

Abstract: This work explores the fiber laser cutting of AISI 431 martensitic steel using an optimized technique of RSM-BBD. A significant increase in gas pressure, power, and cutting speed improved material removal by 62.4%. Surface roughness was reduced by 56.7 percent with decreasing cutting speed, gas pressure, and laser power. The microhardness of the ablated surface was increased due to the resolidification of the molten layer. Surface topography analysis confirmed the machined samples' surface roughness and quality. The research aims to understand AISI 431's machinability and contribute to the improvement of component quality, especially in orthopedic implants and automotive component applications.

Keywords: SS 431; fiber laser; RSM-BBD; surface quality; microhardness; optimization

1. Introduction

A shortage of precision cutting in the manufacturing industry has led to the exploration of advanced techniques such as fiber laser cutting. This machining approach offers exceptional accuracy and versatility, making it particularly appealing for challenging materials like AISI 431 martensitic stainless steel [1]. AISI 431 steel, due to its unique combination of high hardness and corrosion resistance, presents a multitude of advantages for various industrial applications. Its use in aerospace and medical device manufacturing industries is well established, owing to its ability to withstand harsh environments and high mechanical stress [2]. However, its strength and hardness make machining challenging. Traditional cutting methods create rapid tool wear, inaccurate cuts, and heat-affected zones, limiting this remarkable material's use. Machining this material requires a deep understanding of process parameters and optimization. Our experiment involves fiber laser cutting AISI 431 martensitic stainless steel. Response surface methodology with Box—Behnken design (RSM-BBD) optimization is adopted to identify the optimized cutting parameters [3]. Additionally, we conducted microhardness measurements and scanning electron microscope (SEM) analysis to scrutinize the resultant microstructure and mechanical properties of AISI 431 stainless steel. This research will improve the quality and precision of components made from this vital industrial material, advancing the manufacture of medical and aerospace parts.

2. Materials and Methods

2.1. AISI 431 Martensite Alloy and Its Chemical Composition

In this work, AISI 431 steel plate was purchased and cut into 100 mm × 30 mm sizes for fiber laser cutting. Table 1 shows that the chemical composition was initially tested using a positive material identification (PMI) tester.

Table 1. Chemical Composition of AISI 431 alloy.

Weight %	Si	Mn	C	P	S	Cr Ni	Cr	Fe
SS 431	0.83	0.82	0.11	0.03	0.02	2.24	16.41	Bal

2.2. Fiber Laser Machining of AISI 431 Steel

The fiber laser (model: Trumph) was used to machine the SS 431 alloy, with nitrogen as the assist gas. The input parameters of the laser power (P = 2500–3500 W), cutting speed (C_S = 3–5 m/min), and gas pressure (GP = 8–10 bar) were considered in the machining of the AISI 431 alloy. The ranges of the input parameters were determined using the machine restrictions and the accepted literature [4].

2.3. Measurement of MRR, Ra and Microhardness

The weight of SS 431 alloy specimens was evaluated both post and prior machining using a digital weighing balance (least count = 0.001 mg). Each cut was timed during the experiment. The laser-cut sample MRR was determined using Equation (1) [5]. The material removal rate is an essential output characteristic for component manufacturing in all machining areas. Thus, this machining effort sought optimal machining parameters for a higher MRR and lower Ra.

$$MRR \ (\text{mm}^3/\text{min}) \ = \ \frac{W_1 - W_2}{\rho \times t} \times 1000 \tag{1}$$

W_1 and W_2 refer to the initial weight and final weight of the laser-cut sample, and AISI 431 density (ρ) = 7.80 g/cm^3 and the machining time was noted as 't' in minutes. The Ra was measured using the tester SJ-210. The hardness of the sample was measured before and after machining (using the Innova 400 series). The Design Expert software 13.0 was used to optimize experiments with a set of 15 combination values.

3. Results and Discussion

3.1. A Statistical Study of the Material Removal Rate (MRR) on AISI 431 Steel

Laser power (P) vs. cutting speed (C_S) 3D interaction graphs are shown in Figure 1a. The MRR increases from 3.511 to 7.808 mm^3/min when the C_S is set at 5 m/min and the P is altered from 2500 to 3500 W. The nitrogen gas jet expels a lot of molten metal at high power because a high power intensity increases heat flux into the workpiece and melt zone temperature. Laser power significantly affects MRR [6]. A 3D plot of laser power and gas pressure interaction graphs are shown in Figure 1b. The MRR rises from 7.432 to 8.612 mm^3/min when the P is set at 3500 W, and the GP is set at 10. The significant drag force of a high-pressure gas flow increases the maximal material removal rate at high GP [7].
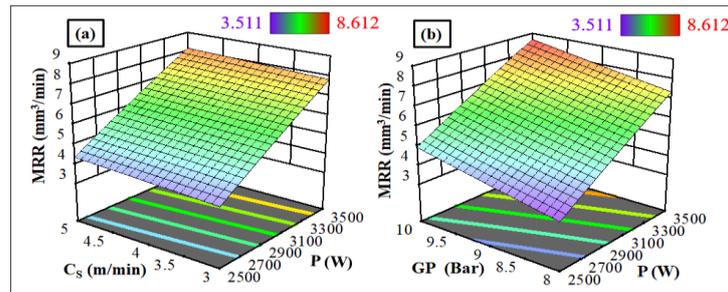
Figure 1. (**a**,**b**) 3D surface plots for MRR.

3.2. A Statistical Study of the Surface Roughness (Ra) on AISI 431 Steel

Figure 2a depicts 3D surface roughness plots as a function of power and cutting speed. When the P and C_S were held at 2500 W and 5 m/min, respectively, the minimum Ra of 2.003 μm was noted. In contrast, a maximum Ra of 6.689 μm was obtained at a power of 3500 W and the same C_S. By raising the C_S and power simultaneously, the laser beam power was considerably enhanced, melting materials quickly and decreasing surface quality [8].
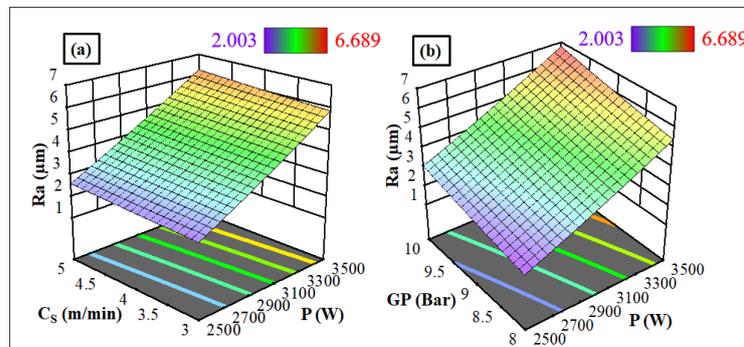

Figure 2. (**a**,**b**) 3D surface plots for Ra.

Figure 2b exhibits power- and GP-dependent 3D surface roughness. With the power and GP at 2500 W and 8 bar, the minimum Ra was 2.003 μm. Adjusting the GP from 8 to 10 bar has minimal impact on machined surface smoothness. A high laser power causes a poor surface finish, extensive striations, resolidified layers, and melted particles [9].

3.3. Parametric Optimization of Fiber Laser Machining

Figure 3a,b display the ideal machined sample's SEM and microhardness graphs. Figure 3a shows the smooth surface with less striation. Similarly, Figure 3b depicts the microhardness of the AISI 431 alloy at different parameters; high-level machining parameters increased the microhardness. Table 2 describes the optimized machining levels with error percentage.
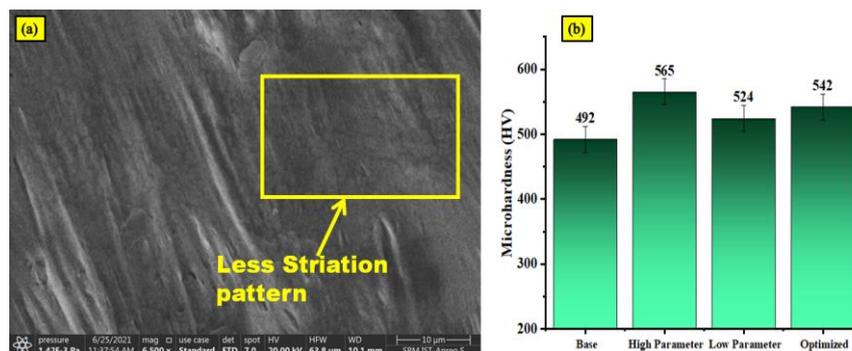

Figure 3. (**a**,**b**) SEM and microhardness graph for optimal machining parameters.

Table 2. The optimum level of fiber laser parameters.

Optimized Parameters			Prediction Values		Experimental Values		% of Error	
P (W)	C_S (m/min)	GP (bar)	MRR (mm^3/min)	Ra (μm)	MRR (mm^3/min)	Ra (μm)	MRR	Ra
3000	3.5	10	6.185	4.187	5.897	3.987	4.65	4.77

Higher laser cutting parameters create more recast layers on the machined workpiece, which cools quicker with nitrogen as the support gas [4]. The recast layer increases the hardness of laser-machined stainless-steel surfaces [9]. An optimal process parameter selection minimizes resolidified layer formation and moderates the microhardness of the AISI 431 alloy.

4. Conclusions

1. An increase in power and cutting speed causes a substantial increase in temperature at the melt surface, leading to the removal of immense amounts of molten material, allowing for a faster material removal rate.
2. Surface roughness increases constantly with the laser cutting speed (C_S) and power (P). A material surface resolidification layer was also visible with increased laser intensity. Therefore, the right power, cutting speed, and gas pressure are needed for surface quality and material removal.
3. When power = 3000 W, C_S = 3.5 m/min, and gas pressure = 10 bar, the optimal set of machining parameters for high MRR and low Ra utilizing the RSM-BBD approach were 6.185 mm^3/min and 4.187 μm, respectively. For AISI 431 steel, fiber laser cutting is the preferable method.

References

1. Figueredo, E.W.A.; Apolinario, L.H.R.; Santos, M.V.; Silva, A.C.S.; Avila, J.A.; Lima, M.S.F. Influence of Laser Beam Power and Scanning Speed on the Macrostructural Characteristics of AISI 316L and AISI 431 Stainless Steel Depositions Produced by Laser Cladding Process. *J. Mater. Eng. Perform.* **2021**, *30*, 3298–3312. [CrossRef]
2. Uddin, M.; Santifoller, R.; Hall, C.; Schlaefer, T. A Grinding-Burnishing Approach to Enhancing Surface Integrity, Tribological, and Corrosion Behavior of Laser-Cladded AISI 431 Alloys. *J. Manuf. Sci. Eng.* **2022**, *144*, 71003. [CrossRef]
3. Balasubramaniyan, C.; Rajkumar, K. Enhancing Low-Speed WEDM Machining Capabilities on Nitronic-50 with a Constant Frequency Ultrasonic Hybrid Method. *Proc. Inst. Mech. Eng. Part C J. Mech. Eng. Sci.* **2023**. [CrossRef]
4. Balasubramaniyan, C.; Rajkumar, K.; Santosh, S. Fiber Laser Cutting of Cu–Zr Added Quaternary NiTi Shape Memory Alloy: Experimental Investigation and Optimization. *Arab. J. Sci. Eng.* **2023**, *48*, 3665–3679. [CrossRef]
5. Balasubramaniyan, C.; Rajkumar, K.; Santosh, S. Wire-EDM Machinability Investigation on Quaternary Ni$_{44}$Ti$_{50}$Cu$_4$Zr$_2$ Shape Memory Alloy. *Mater. Manuf.* **2021**, *36*, 1161–1170. [CrossRef]
6. Arun, A.; Rajkumar, K.; Santosh, S. Fiber Laser Cutting Study on Ternary NiTiV Shape Memory Alloy. *Mater. Manuf.* **2023**, *38*, 1745–1754. [CrossRef]

7. Santosh, S.; Kevin Thomas, J.; Pavithran, M.; Nithyanandh, G.; Ashwath, J. An Experimental Analysis on the Influence of CO2 Laser Machining Parameters on a Copper-Based Shape Memory Alloy. *Opt. Laser Technol.* **2022**, *153*, 108210. [CrossRef]
8. Santosh, S.; Srivatsan, S.; Vignesh Pandian, R. Unravelling the effect of CO_2 laser machining parameters on the surface and shape memory characteristics of CuAlFeMn quaternary shape memory alloy. *Opt. Laser Technol.* **2023**, *163*, 109306. [CrossRef]
9. Balasubramaniyan, C.; Santosh, S.; Rajkumar, K. Surface Quality and Morphology of NiTiCuZr Shape Memory Alloy Machined Using Thermal-Energy Processes: An Examination of Comparative Topography. *Surf. Topogr.* **2022**, *10*, 035019. [CrossRef]